Supporting Information

Molecular Dynamics Studies on the Lithium Ion Conduction Behaviors Depending on Tilted Grain Boundaries with various symmetries in Garnet-Type $Li_7La_3Zr_2O_{12}$

Hiromasa Shiiba[1], Nobuyuki Zettsu[*1,2], Miho Yamashita[1], Hitoshi Onodera[1], Randy Jalem[3,4], Masanobu Nakayama[3,4,5], and Katsuya Teshima[*1,2]

[1] Department of Materials Chemistry, Faculty of Engineering, Shinshu University, 4-17-1 Wakasato, Nagano 380-8553, Japan.

[2] Center for Energy and Environmental Science, Shinshu University, 4-17-1 Wakasato, Nagano 380-8553, Japan.

[3] Global Research Center for Energy Based Nanomaterials Science (GREEN), National Institute for Materials Science Tsukuba, Ibaraki 305-0047.

[4] Materials research by Information Integration" Initiative (Mi[2]i), National Institute for Materials Science Tsukuba, Ibaraki 305-0047.

[5] Frontier Research Institute for Materials Science (FRIMS), Nagoya Institute of Technology, Gokiso, Showa, Nagoya, Aichi 466-8555, Japan.

Results

After fitting the high-temperature region of the computationally predicted LLZO conductivity plot, the extrapolation to a temperature of 300 K resulted in a total conductivity of 32.9 mS/cm, which was two orders of magnitude higher than the bulk conductivity determined in the experimental studies. In addition, the bulk conductivities calculated along the *a*, *b*, and *c* axes were 29.5, 40.0, and 31.5 S/cm, respectively, indicating that the differences between them were negligible and that the results reported in this work were identical to the isotropic ion conducting characteristics of cubic LLZO. Furthermore, the calculated bulk lattice parameter at 300 K (12.92(1) Å) differed from the corresponding experimental value (12.98 Å[1]) by less than 1%. Therefore, the optimized lattice parameter value was used in the MD simulations, which allowed statistical evaluation of the Li conducting behavior of cubic LLZO (similar results were obtained in our previous *ab initio* MD study of LLZO[2]).

References

1. Awaka, J.; Takashima, A.; Kataoka, K.; Kijima, N.; Idemoto, Y.; Akimoto, J. Crystal Structure of Fast Lithium-ion-conducting Cubic $Li_7La_3Zr_2O_{12}$. *Chem. Lett.* **2011**, 40, 60-62.
2. Jalem, R.; Yamamoto, Y.; Shiiba, H.; Nakayama, M.; Munakata, H.; Kasuga, T.; Kanamura, K. Concerted Migration Mechanism in the Li Ion Dynamics of Garnet-Type $Li_7La_3Zr_2O_{12}$. *Chem. Mater.* **2013**, 25, 425-430.

Table S1. Li occupancies of the 24d and 48g/96h sites in cubic and tetragonal LLZO obtained through NPT simulations for 20 ps.

	Li occupancy	
	24d	48g/96h
Cubic	0.617	0.858
Tetragonal	0.622	0.856

Table S2. Fitted local Li ionic conductivity across the GB layer at 300 K and activation energies derived from the MSD analysis.

	σ (S cm^{-1}) (at 300 K)	Activation energy (eV)
Bulk	3.3×10^{-2}	0.18
Σ3 (2-1-1)=(1-21)	8.0×10^{-6}	0.41
Σ3 (100) × (2-12)	5.4×10^{-6}	0.44
Σ3 (1-10)=(0-11)	1.8×10^{-4}	0.32
Σ3 (110) × (411)	1.6×10^{-4}	0.33
Σ5 (031)=(03-1)	5.0×10^{-4}	0.31
Σ7 (3-2-1)=(2-31)	4.0×10^{-4}	0.31
Σ9 (1-14)=(-114)	2.0×10^{-3}	0.26
Σ11 (1-13)=(-113)	1.4×10^{-3}	0.27

Table S3. Parameters of the Buckingham interionic potentials.

Interaction	A_{ij} (eV)	ρ_{ij} (Å)	C_{ij} (eV Å^6)
$Li^{0.7+}$ - $O^{1.4-}$	876.86	0.2433	0
$La^{2.1+}$ - $O^{1.4-}$	14509.63	0.2438	30.83
$Zr^{2.8+}$ - $O^{1.4-}$	1366.09	0.3181	0
$O^{1.4-}$ - $O^{1.4-}$	4869.99	0.2402	27.22

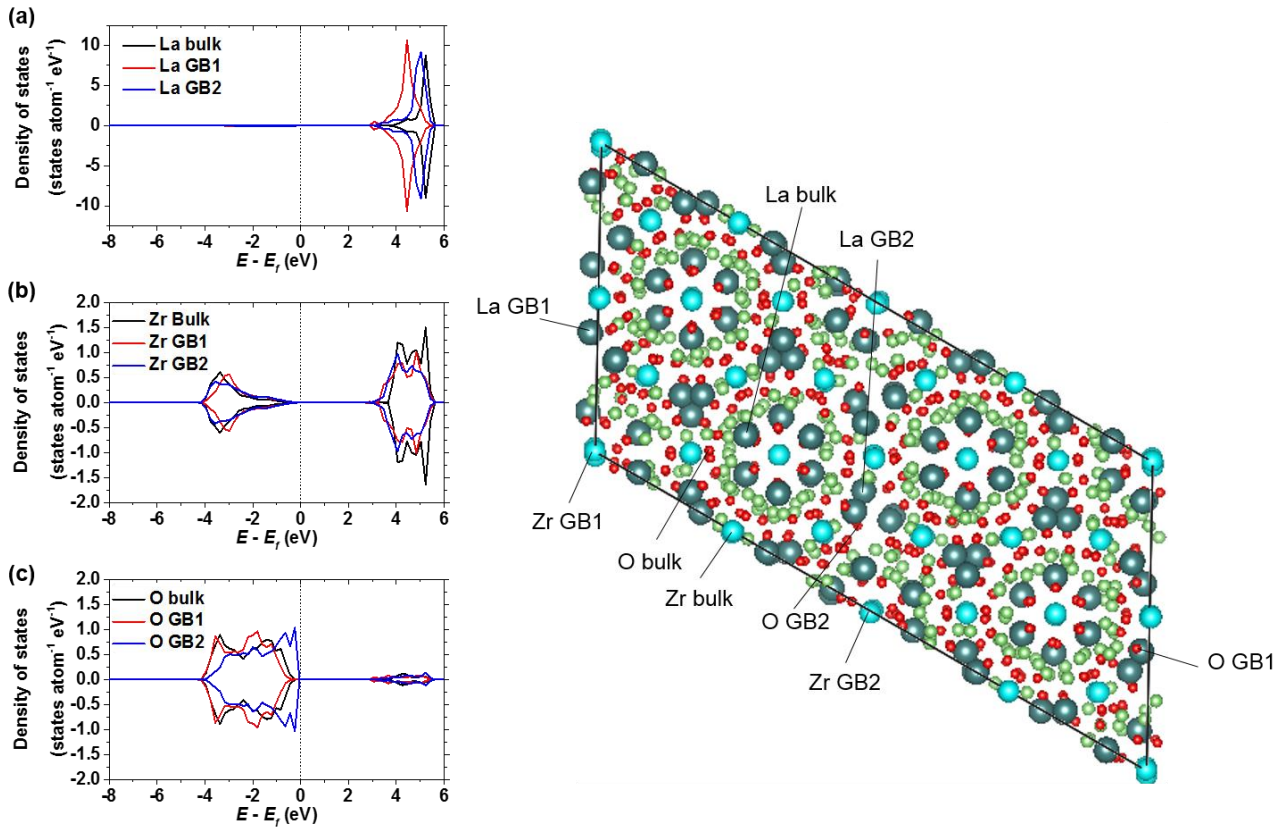

Figure S1. Partial densities of states calculated for the (a) La-4f, (b) Zr-4d, and (c) O-2p bands of the Σ3 (2-1-1)=(1-21) GB model in the bulk and GB regions.

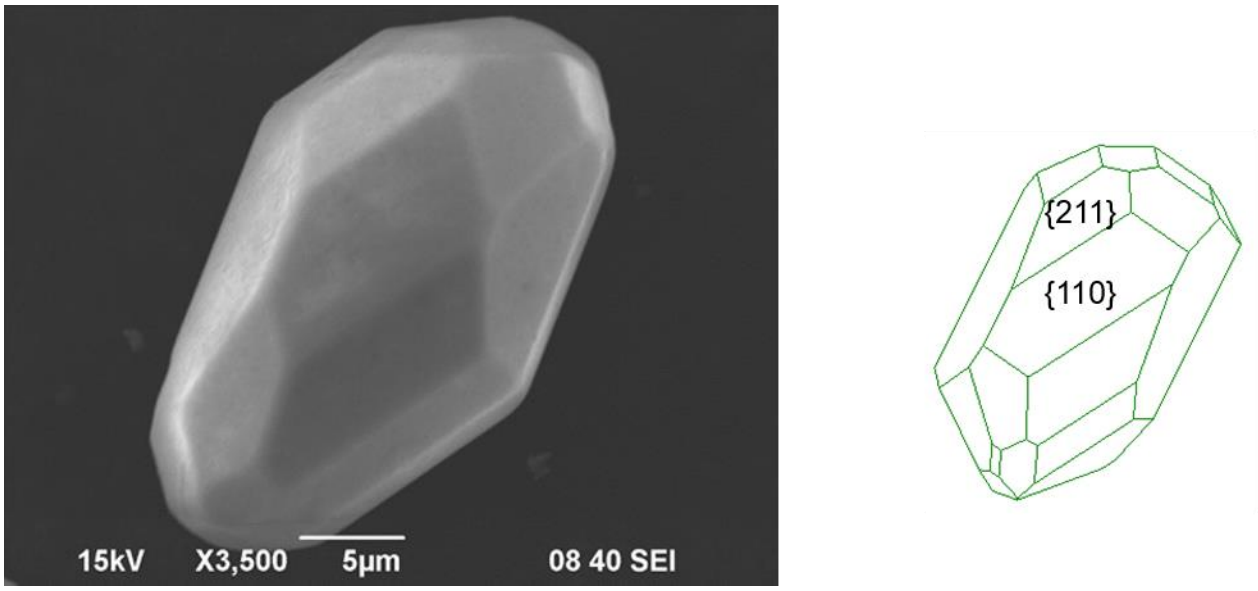

Figure S2. SEM images of a typical $Li_7La_3Zr_2O_{12}$ crystal grown using a LiOH flux.

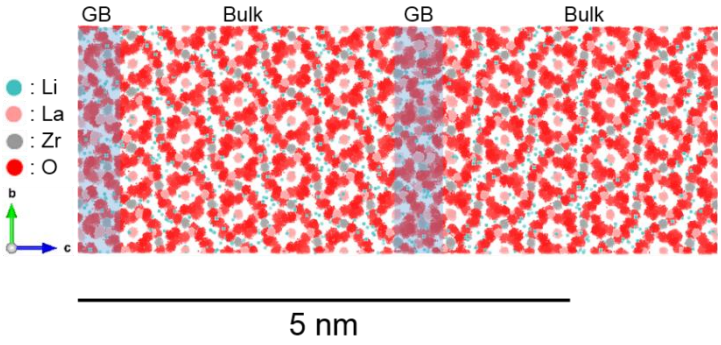

Figure S3. Trajectories of La, Zr, and O atoms obtained for the Σ3 (2-1-1)=(1-21) GB models at 1300 K.

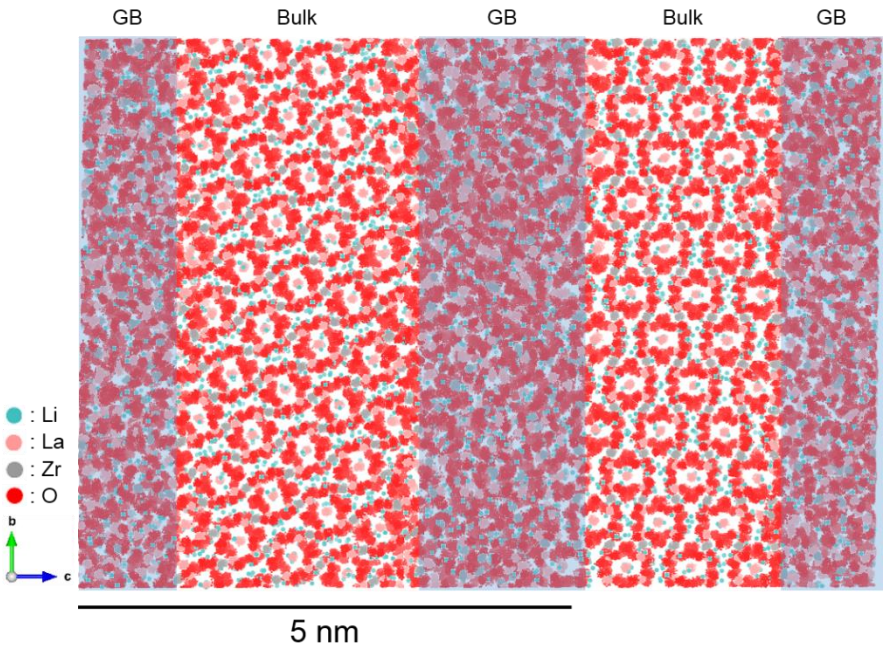

Figure S4. Trajectories of La, Zr, and O atoms obtained for the Σ3 (100)×(2-12) GB models at 1300 K.

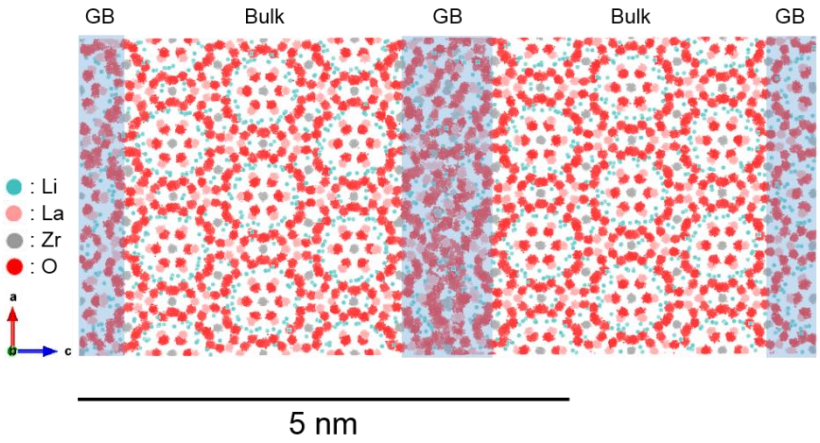

Figure S5. Trajectories of La, Zr, and O atoms obtained for the Σ3 (1-10)=(0-11) GB models at 1300 K.

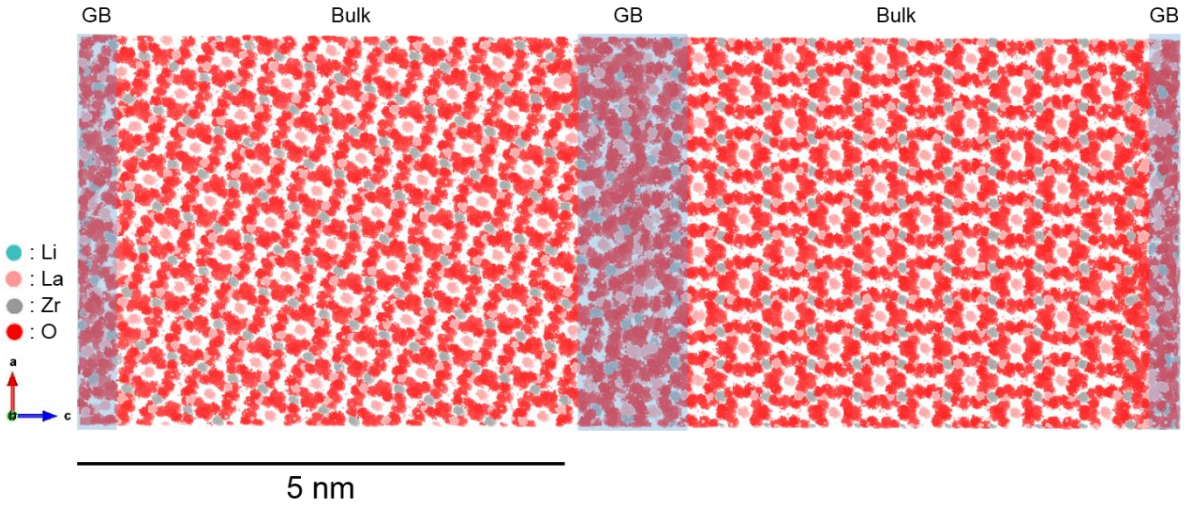

Figure S6. Trajectories of La, Zr, and O atoms obtained for the (d) Σ3 (110)×(411) GB models at 1300 K.

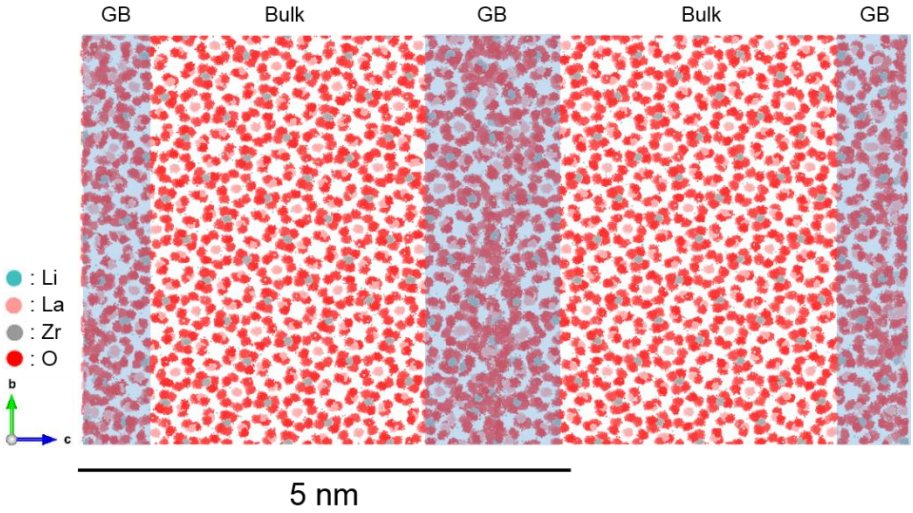

Figure S7. Trajectories of La, Zr, and O atoms obtained for the Σ5 (031) = (03-1) GB models at 1300 K.

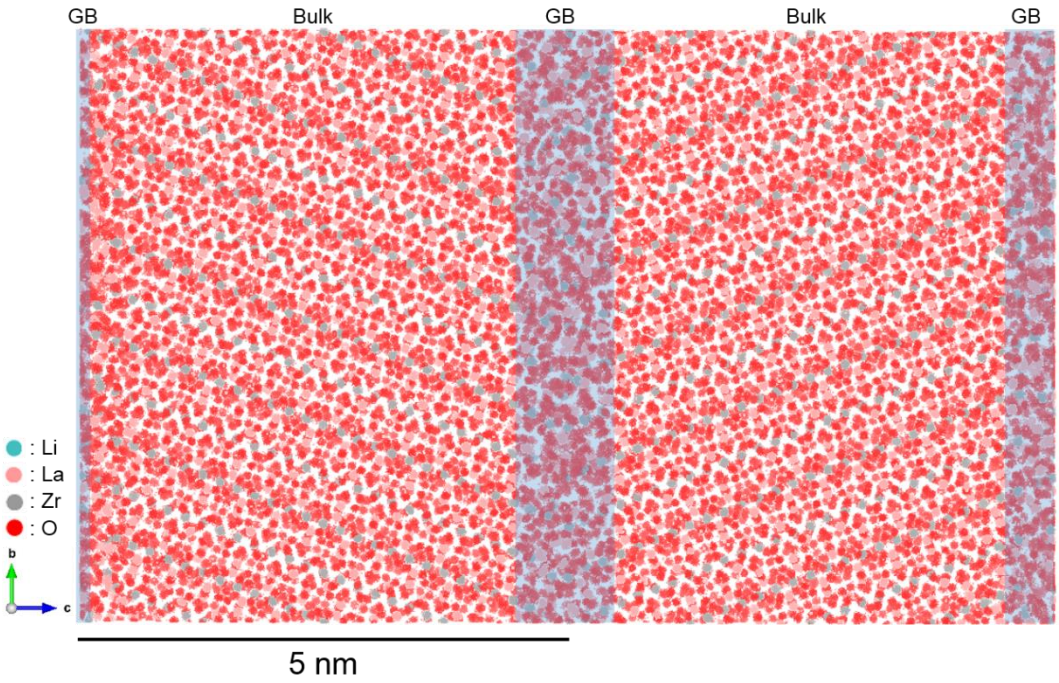

Figure S8. Trajectories of La, Zr, and O atoms obtained for the Σ7 (3-2-1) = (2-31) GB models at 1300 K.

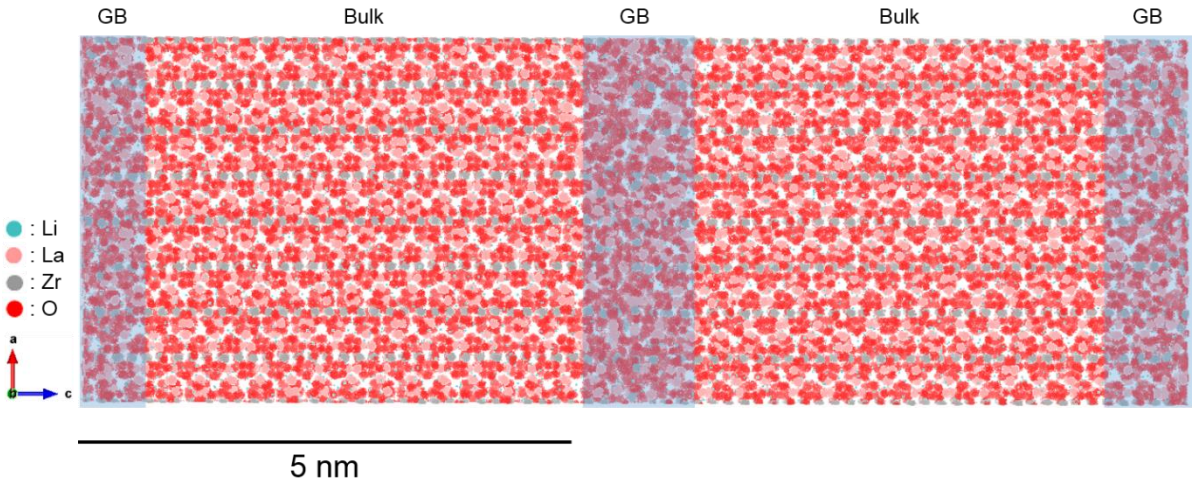

Figure S9. Trajectories of La, Zr, and O atoms obtained for the Σ9 (1-14) = (-114) GB models at 1300 K.

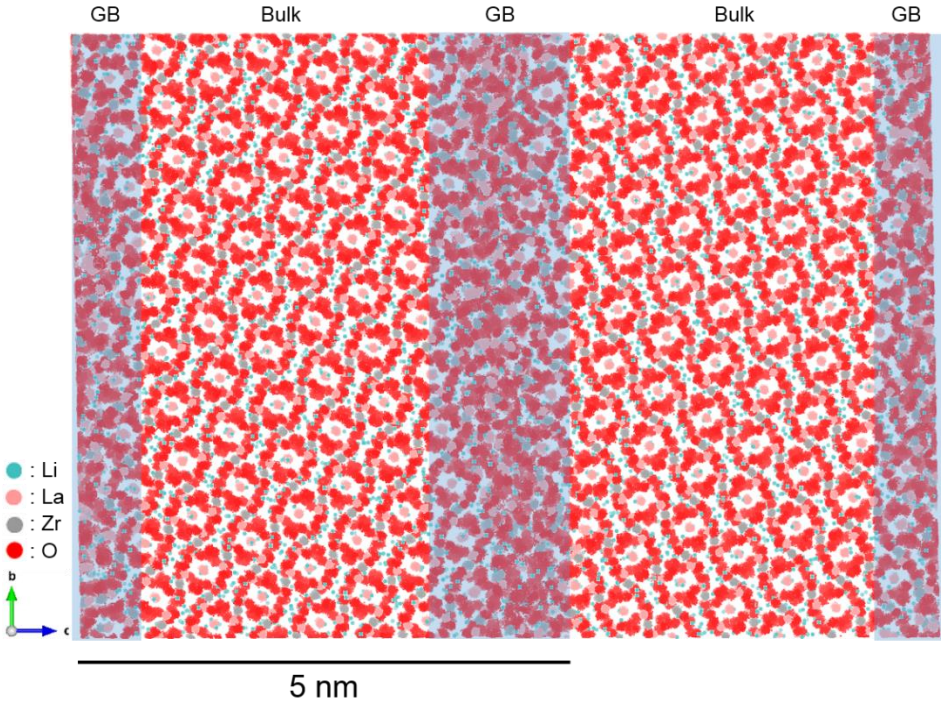

Figure S10. Trajectories of La, Zr, and O atoms obtained for the Σ11 (1-13) = (-113) GB models at 1300 K.

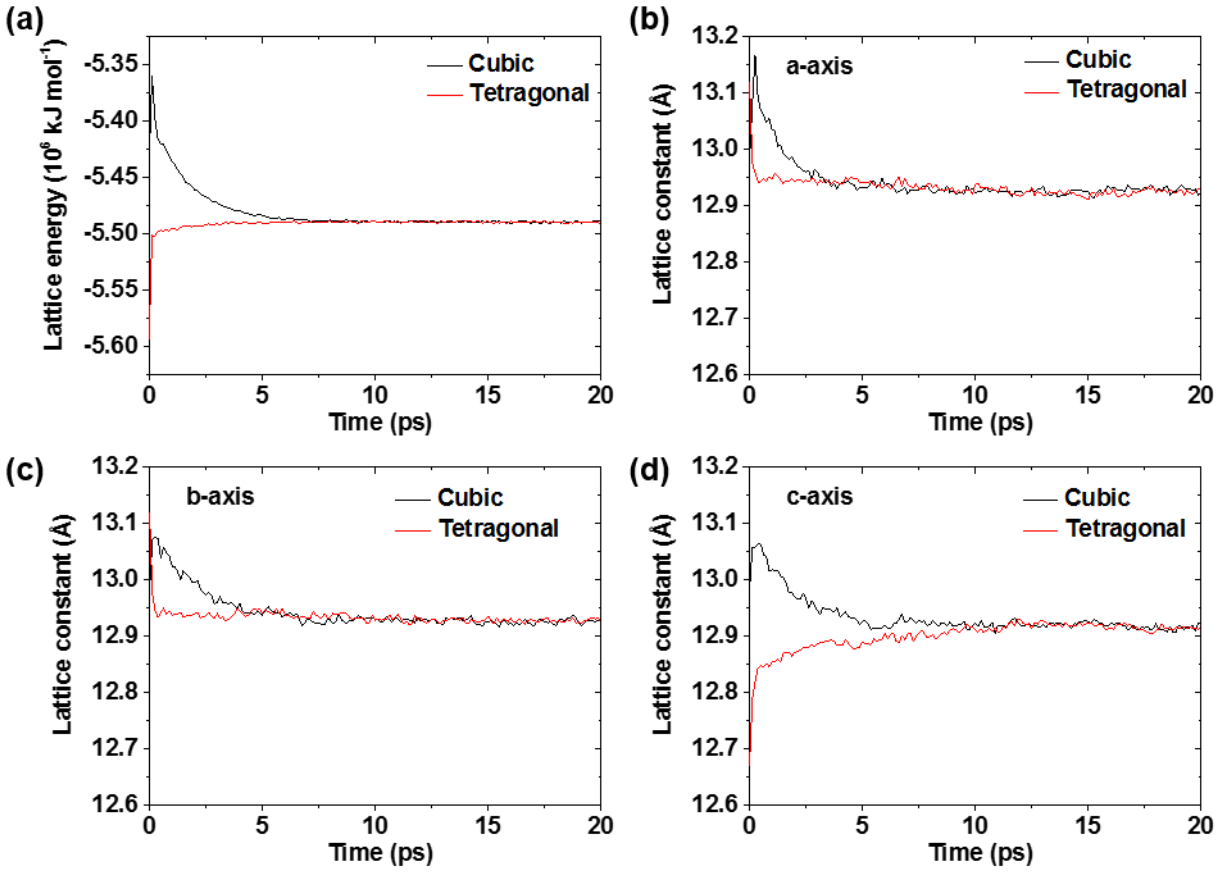

Figure S11. Variations of the (a) lattice energies and lattice constants along the (b) *a*, (c) *b*, (d) and *c* axes of LLZO with the cubic and tetragonal initial lattices as functions of time.

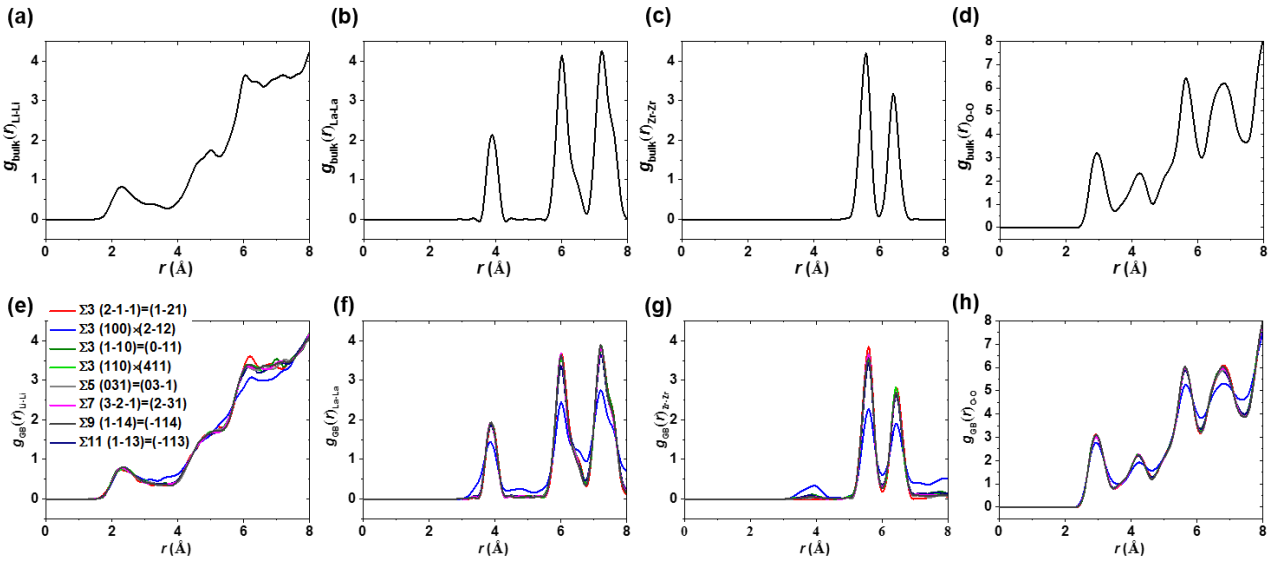

Figure S12. RDFs plotted for the Li–Li, La–La, Zr–Zr, and O–O interactions of the (a–d) bulk and (e–h) GB models.

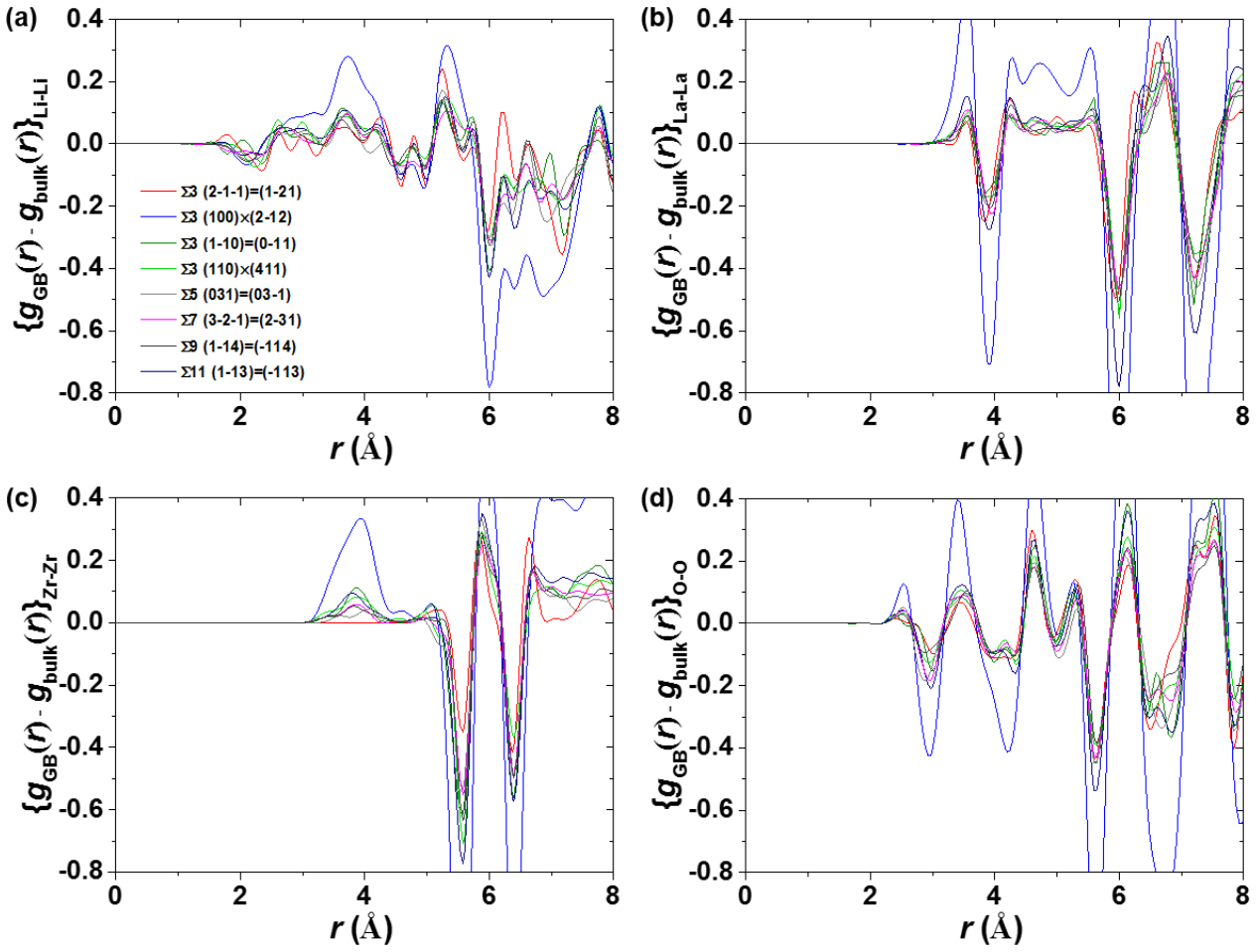

Figure S13. RDF differences between the bulk and GB models calculated for the Li–Li, La–La, Zr–Zr, and O–O interactions.

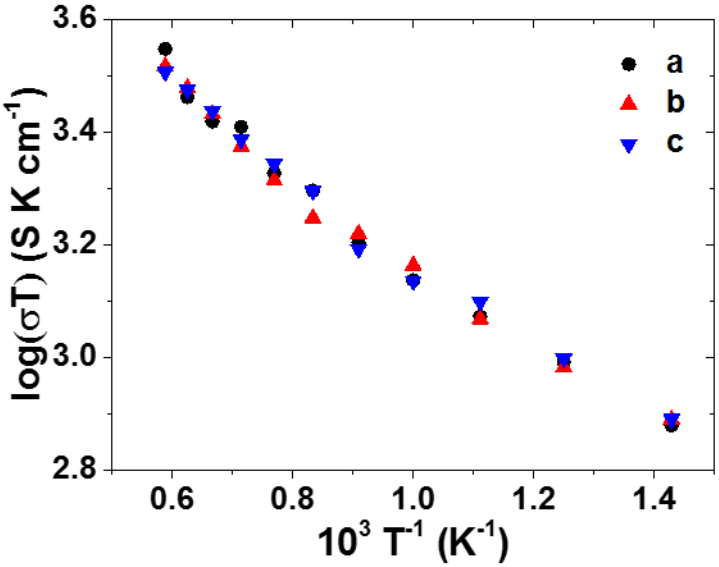

Figure S14. Arrhenius plots of the Li ionic conductivity constructed for the isotropic 3D Li diffusion path in the bulk garnet LLZO along the *a*, *b*, and *c* axes.

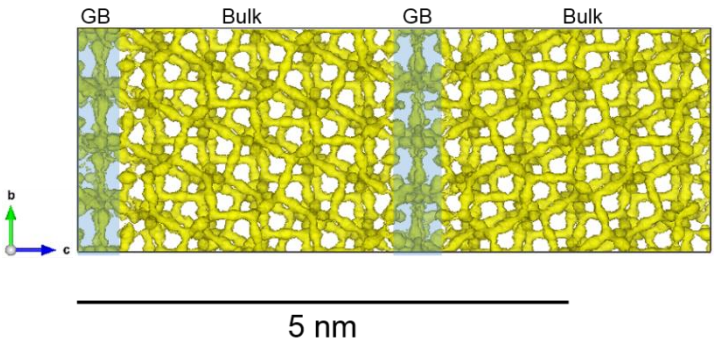

Figure S15. Li ion trajectories obtained for the Σ3 (2-1-1)=(1-21) GB models at 1300 K.

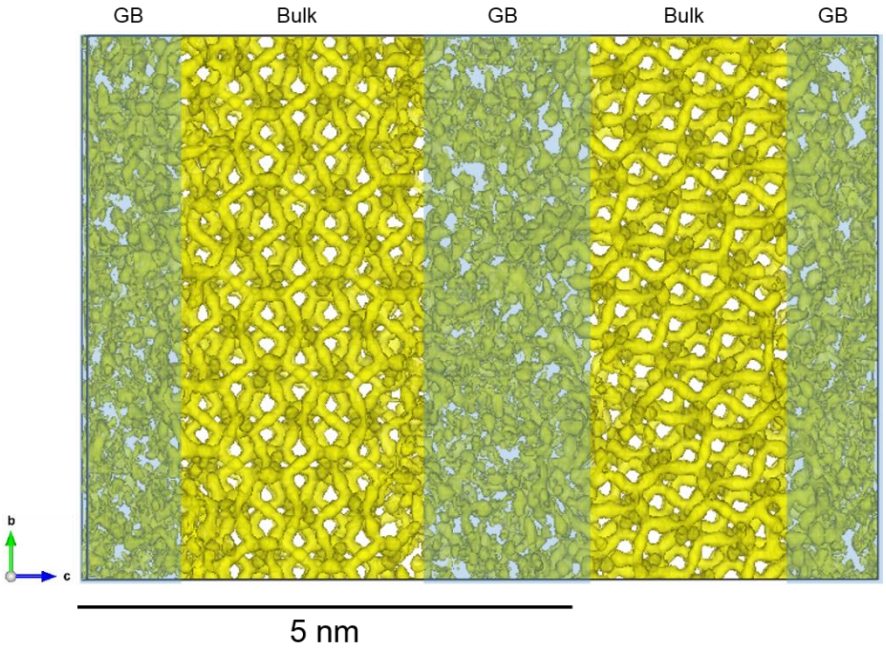

Figure S16. Li ion trajectories obtained for the Σ3 (100)×(2-12) GB models at 1300 K.

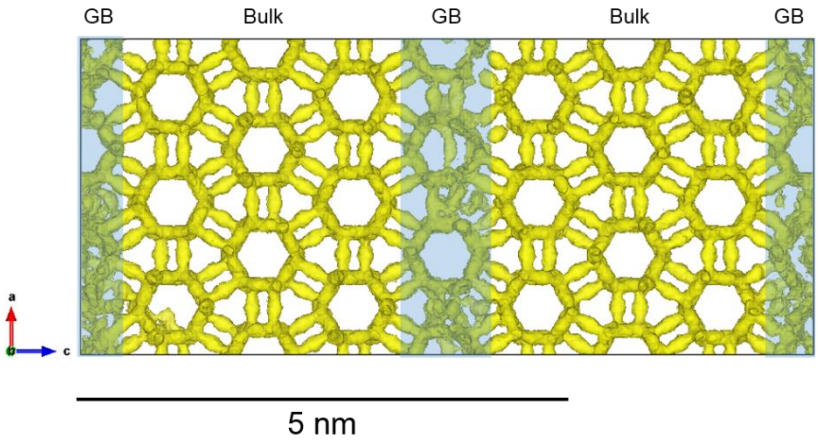

Figure S17. Li ion trajectories obtained for the Σ3 (1-10)=(0-11) GB models at 1300 K.

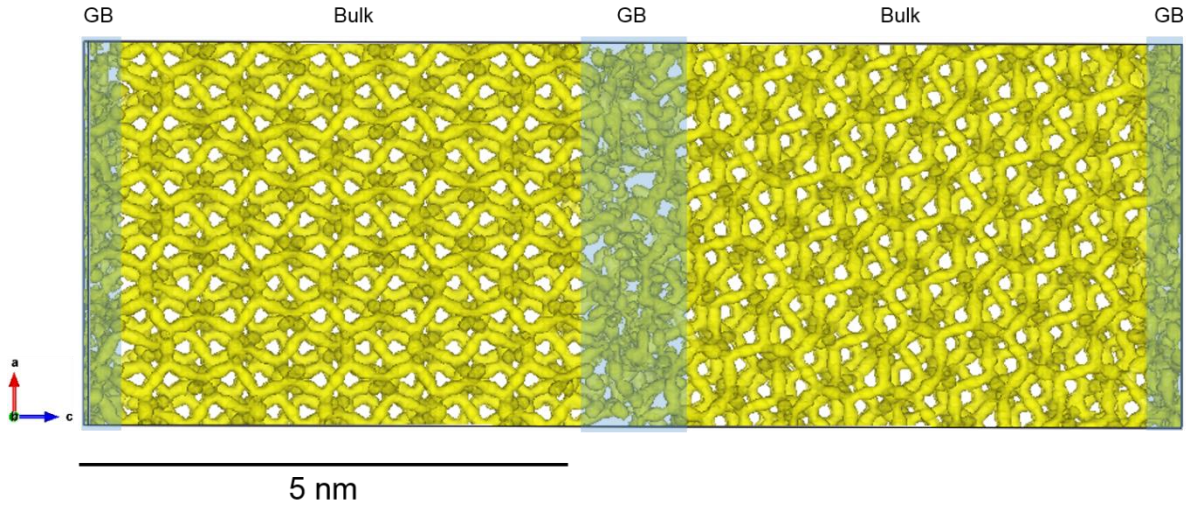

Figure S18. Li ion trajectories obtained for the Σ3 (110)×(411) GB models at 1300 K.

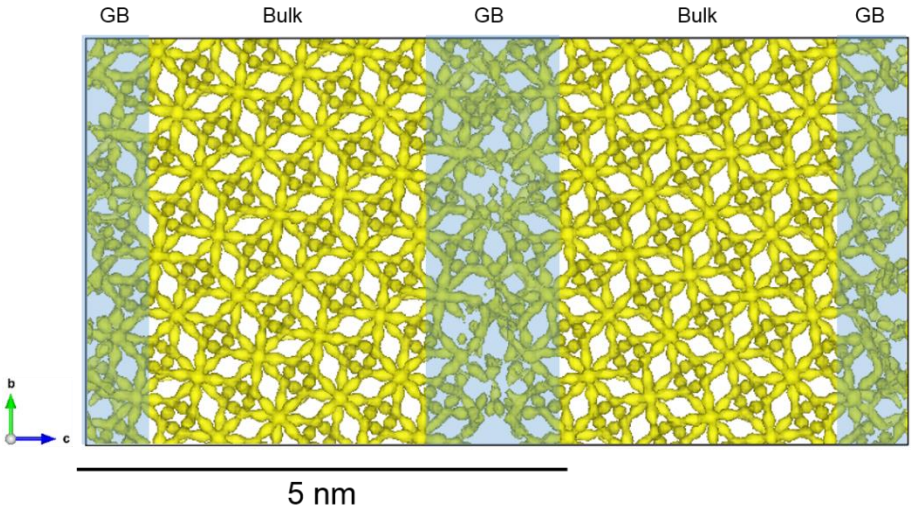

Figure S19. Li ion trajectories obtained for the Σ5 (031) = (03-1) GB models at 1300 K.

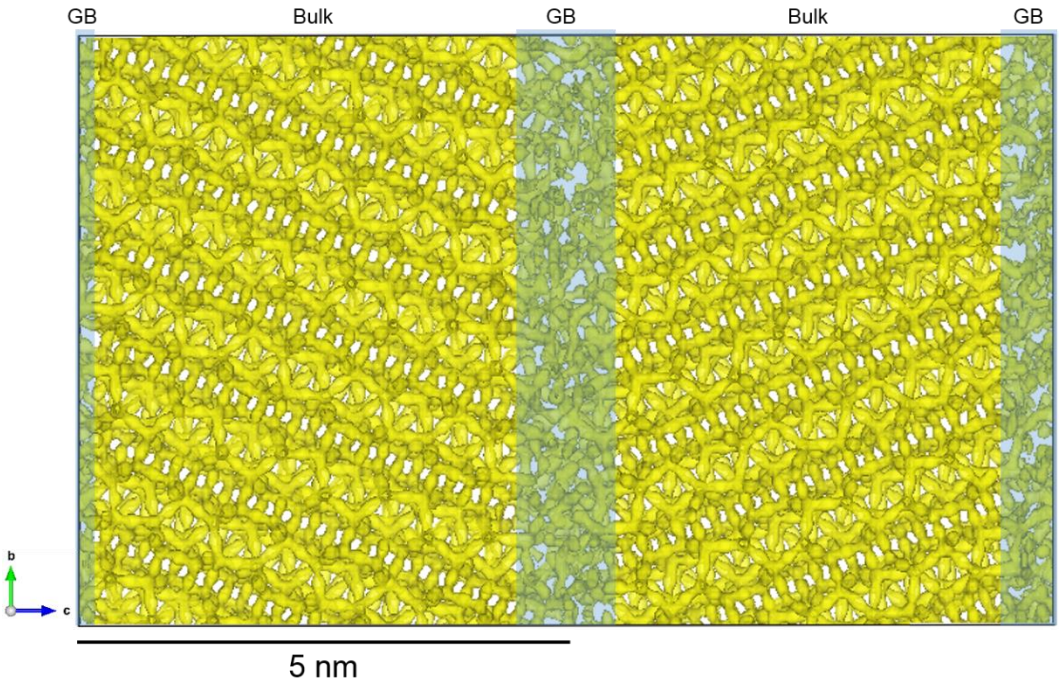

Figure S20. Li ion trajectories obtained for the Σ7 (3-2-1) = (2-31) GB models at 1300 K.

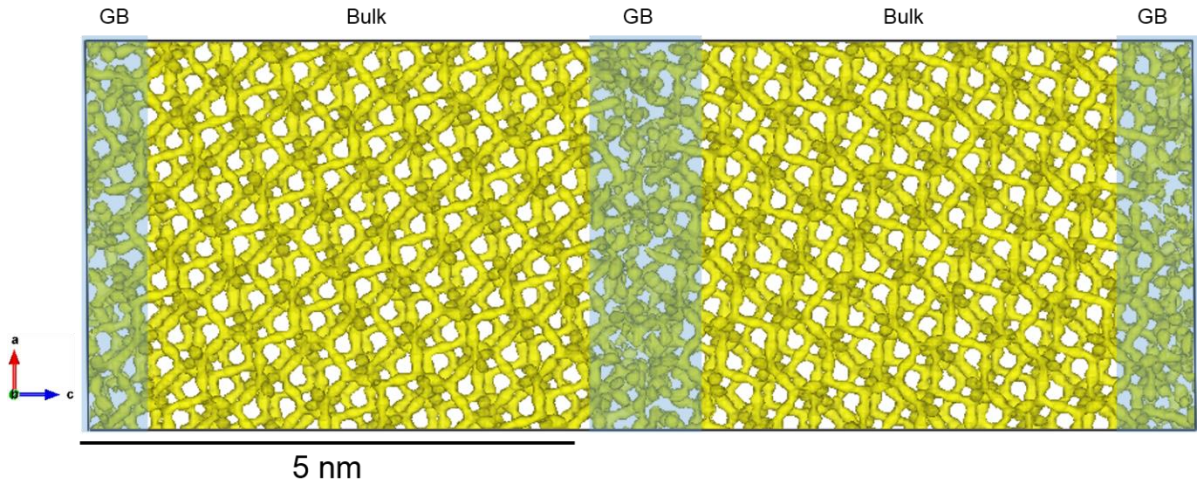

Figure S21. Li ion trajectories obtained for the Σ9 (1-14) = (-114) GB models at 1300 K.

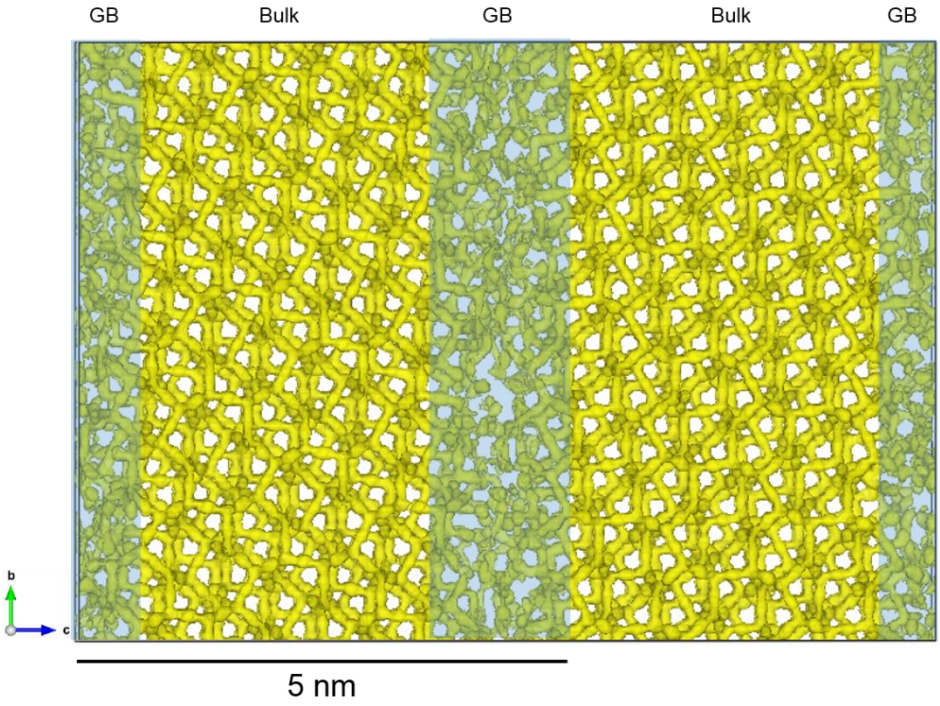

Figure S22. Li ion trajectories obtained for the Σ11 (1-13) = (-113) GB models at 1300 K.